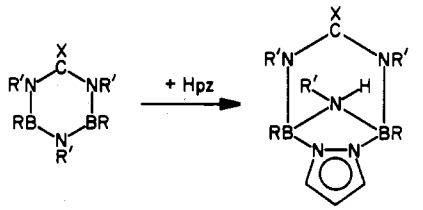

(4)

I 4

a: R = C_2H_5; R′ = CH_3; X = O
c: R = R′ = CH_3; X = S
d: R = CH_3; R′ = C_2H_5; X = S
e: R = C_6H_5; R′ = CH_3; X = S

by the reaction of the recently described[20] triply bridged diboron species J with Hpz under displacement of one *N,N′*-dimethylurea moiety as shown in eq 5.

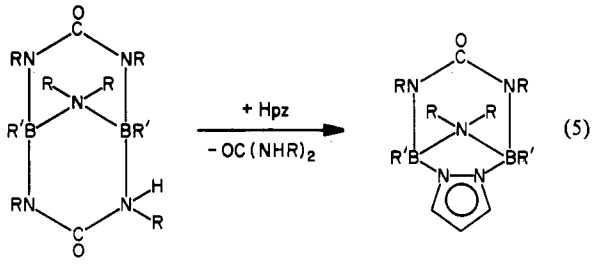

(5)

J 4b: R = CH_3; R′ = C_2H_5

The compounds of type **4** are the first representatives of a novel type of relatives of the pyrazaboles that may be illustrated in general form by **5**. Species of type **5** are related to triply bridged pyrazaboles of type **2**, in which one bridging pz group has then been replaced by another bridging moiety, just as in species of type **3** one of the bridging pz groups of **1** has been replaced by another bridging group.

Discussion

The present data suggest that when pyrazole (=Hpz) interacts

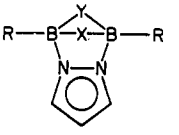

5

with heterocycles containing two annular boron atoms, the NH moiety of Hpz seeks out the most basic site of the ring. Whenever possible, the pyrazolyl nitrogens will attach to the boron atoms, but the nature of the ultimate product is a function of the specific reaction conditions, primarily the ratio of the reactants and the temperature. These can lead to a complete breakdown of the original heterocycle to yield amine–borane type adducts of (1-pyrazolyl)boranes as examplified by **6**. Alternatively, fragments of the original ring systems are retained, leading to pyrazaboles of type **2** or the pyrazabole relatives of types **3** or **4**, respectively.

The ring system of general formula **5** is a novel type which is specifically related to the triply bridged pyrazaboles of type **2**. Hence, it is not surprising that under forcing conditions and in the presence of sufficient Hpz, **5** converts to pyrazaboles of type **1** (with R = pz). In general, the latter seem to be the thermodynamically favored products in reactions of boron derivatives with Hpz. Consequently, species of type **3** can also be converted to those of type **1**.

Although at this time compounds of type **3** are limited to those where X is an amino or a chalcogenyl group and those of type **5** to species where X is an amino group and Y a bridging urea moiety, it is reasonable to assume that compounds containing bridging groups X and Y other than those cited will also become available.

Acknowledgment. This work was supported by the Office of Naval Research (K.N.) and the Fonds der Chemischen Industrie (A.M.). Travel funds from the Alexander von Humboldt Foundation (K.N.) and the North Atlantic Treaty Organization (A.M. and K.N.) are also gratefully acknowledged.

Contribution from AT&T Bell Laboratories,
Murray Hill, New Jersey 07974

A Study of the ^{13}C Chemical Shift Anisotropy in Metal Acetylides

T. M. Duncan

Received January 12, 1989

The anisotropy of the ^{13}C chemical shielding in five metal acetylides, Li_2C_2, Na_2C_2, CaC_2, SrC_2, and BaC_2, is measured with ^{13}C nuclear magnetic resonance (NMR) spectroscopy. The chemical shift anisotropies of the acetylides range from 180 to 235 ppm, compared to 160 ppm for HC≡CH. The shielding perpendicular to the C≡C bond in the acetylides is invariant with cation and is ~315 ppm, relative to TMS. However, the shielding parallel to the C≡C bond varies by over 110 ppm and correlates with the distances to cations in the plane bisecting the C≡C bond. For compounds with bonding along the C≡C axis (the alkaline-earth-metal acetylides and acetylene) the isotropic shift is proportional to the acetylide–nearest-neighbor distance and the ionization potential of the nearest neighbor. The spectral broadening in the ^{13}C NMR spectra of the alkaline-earth-metal acetylides decreases and the isotropic shift moves to higher frequency as the size of the cation increases. Both trends are attributed to the paramagnetic component of the shielding, relative to a gauge origin at the carbon nucleus.

Introduction

The anisotropy of the chemical shielding at a nucleus is of fundamental and practical interest. It offers, for example, the intrinsic merit of characterizing chemical bonding; chemical shift anisotropy, and especially the identification of the diamagnetic and paramagnetic contributions for a given gauge origin, can be used to corroborate calculations of electronic wave functions. It also has potential for chemical analysis of solid samples; the chemical shift anisotropy differentiates between similar species of a carbon functionality when the isotropic shift may show no trend. Discussions of the trends in ^{13}C chemical shift anisotropies are offered in a recent review[1] and a compilation.[2] Although ab initio calculations of chemical shift anisotropies are improving, chemical analysis of solids is almost exclusively by comparison to the spectra of reference compounds. However, there is a lack of reference data; for acetylenic carbons the chemical shift anisotropy has been reported for only four compounds.[2] The principal components of the ^{13}C shielding tensor for five inorganic acetylides are reported here. Furthermore, trends within the compounds

(1) Veeman, W. S. *Prog. NMR Spectrosc.* **1984**, *16*, 193.
(2) Duncan, T. M. *J. Phys. Chem. Ref. Data* **1987**, *16*, 125.

0020-1669/89/1328-2663$01.50/0

Table I. Crystallographic Parameters of Metal Acetylides

compd	lattice params, Å			C≡C dist, Å	structure	ref
	a	*b*	*c*			
Li_2C_2	3.65	5.44	4.83	1.20	orthorhombic (D_{2h}^{25}-*Immm*)	7
Na_2C_2	6.743		12.674	1.200 (6)	tetragonal (D_{4h}^{20}-$I4_1/acd$)	8
CaC_2	3.87		6.37	1.191 (9)	tetragonal (D_{4h}^{17}-$I4/mmm$)	3–5
SrC_2	4.11		6.68	1.19[a]	tetragonal (D_{4h}^{17}-$I4/mmm$)	3–5
BaC_2	4.39		7.04	1.19[a]	tetragonal (D_{4h}^{17}-$I4/mmm$)	3–5

[a] Experimental distances not reported: estimated distances (see ref 3).

and correlations to other physical properties are discussed.

The ionic carbides of the alkali and alkaline-earth metals exist as discrete $(C{\equiv}C)^{2-}$ anions coordinated to metal anions.[3,4] The carbon–carbon bonding in acetylides is similar to that in alkynes, having a bond length of 1.19 Å compared to 1.205 Å for C_2H_2. Although the structures of these metal acetylides are similar, there are subtle variations as shown in Figure 1. A major difference between the structures of the alkali-metal acetylides (Li_2C_2 and Na_2C_2) and the alkaline-earth-metal acetylides (CaC_2, SrC_2, and BaC_2) is the position of the cation relative to the $(C{\equiv}C)^{2-}$ bond. Some cations in the alkaline-earth-metal acetylides lie on the $(C{\equiv}C)^{2-}$ axis[3-2] whereas no cations in the alkali-metal acetylides lie on the axis.[7,8] In addition, the structures of Li_2C_2 and Na_2C_2 differ in the relative arrangement of the acetylide units. The $(C{\equiv}C)^{2-}$ units of Li_2C_2 lie parallel along the *c* axis[6,7] whereas successive $(C{\equiv}C)^{2-}$ units along the *c* axis in Na_2C_2 are rotated 90°.[8] However, all $(C{\equiv}C)^{2-}$ bonds in Na_2C_2 lie in a plane perpendicular to the *c* axis.[8] The spiral configuration of the $(C{\equiv}C)^{2-}$ units displaces the Na cations (indicated by the positions above and below the half-unit cell in Figure 1), and Na_2C_2 has a distorted CaF_2-like structure.[8]

Initial ^{13}C NMR studies of the acetylenic group concerned the isotropic shift of organic alkyls.[9,10] The isotropic shifts of acetylenic groups as a whole occurred between those of olefinic and paraffinic carbons, contrary to the trend that increasing p character caused shifts to higher frequency.[9] Furthermore, the isotropic shifts spanned a comparatively narrow range and were not correlated to the electronegativities of nearest-neighbor substituents, as they were in olefinic and paraffinic carbons.[10] The principal components of the ^{13}C chemical shift of the acetylenic groups have been reported subsequently for acetylene,[11] diacetylene,[12] propyne,[13] and 2-butyne.[14] The differences in chemical shielding perpendicular and parallel to the $(C{\equiv}C)^{2-}$ bond are uniformly about 225 ppm for these compounds. Moreover, for acetylenic carbon bonded to hydrogen, the shielding parallel to the triple bond reaches the extreme for diamagnetic compounds (~−90 ppm, relative to tetramethylsilane) as expected for linear species.[13] Three metal acetylides (CaC_2[15] and ThC_2 and UC_2[16]) have been examined with ^{13}C NMR spectroscopy, but the chemical shielding anisotropies were not reported.

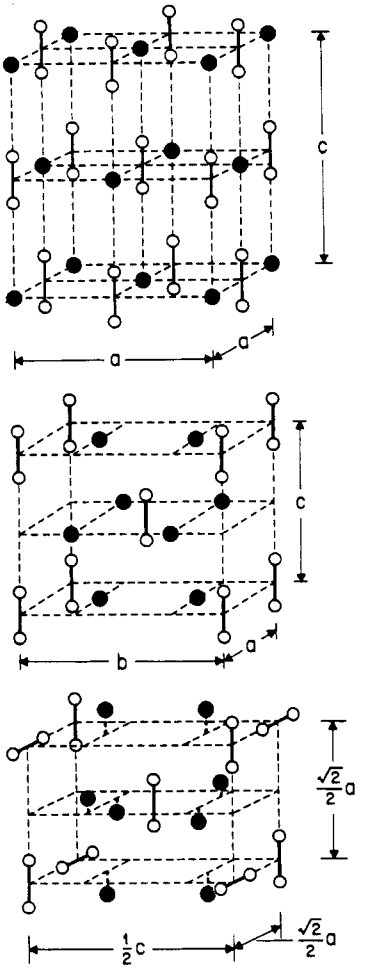

Figure 1. Three structures of metal acetylides: the tetragonal lattice of CaC_2, SrC_2, and BaC_2[3,4] (top), the Rb_2O_2-type[6] lattice of Li_2C_2[7] (middle), and the distorted-CaF_2 lattice of Na_2C_2[8] (bottom). Each structure is drawn with a vertical acetylide ion at the center. Table I contains the lattice constants of each acetylide.

Experimental Procedures

Samples of the five acetylides were obtained from Alfa Products in the following particle sizes: Li_2C_2, −325 mesh; Na_2C_2 and BaC_2, powder; SrC_2, −8 mesh; CaC_2, lumps (~1 mm). For each compound, the average radius of the particles was less than the skin depth of the rf radiation. Li_2C_2, BaC_2 and SrC_2 were 99% pure, whereas Na_2C_2 contained up to 20% NaC_2H and CaC_2 contained up to 20% CaO. Because the acetylides are highly reactive, the compounds were handled and sealed in dry nitrogen. [Prolonged exposure of some acetylides to N_2 yields inorganic cyanides such as $Ba(CN)_2$[1]. The ^{13}C NMR spectra were obtained within 2 weeks after the samples were exposed to N_2.] The cylindrical NMR samples (10-mm diameter, 25-mm length) contained from 1.5×10^{20} to 3.0×10^{20} ^{13}C nuclei.

The NMR experiments were performed on a Bruker CXP-200 spectrometer at 50.35 MHz. The ^{13}C NMR spectra were obtained by Fourier-transforming the accumulation of typically 100–500 quadrature-detected free-induction decays observed immediately after 90° pulses. On alternate cycles, a 180° prepulse was applied at a time τ before the 90° pulse, and alternate decays were negated before addition to the accumulation. The delay τ between the 180° and 90° pulses was always set longer than the spin–spin relaxation time (T_2) and shorter than the spin–lattice relaxation time (T_1). The T_1's were estimated by observing the decrease in the intensity of the NMR signal as a function of the time interval between successive cycles (saturation-recovery technique).[17] The chemical shift parameters are reported on the δ scale, relative to tetramethylsilane (TMS). That is, higher frequency is to the

(3) Klug, H. P.; Brasted, R. C. *Comprehensive Inorganic Chemistry*; Pergamon: New York, 1973; Vol. 7, pp 1203–1207.
(4) Wells, H. P. *Structural Inorganic Chemistry*, 4th ed.; Oxford: London, 1975; pp 756–761.
(5) Atoji, M.; Medrud, R. C. *J. Chem. Phys.* **1959**, *31*, 332.
(6) Föppl, H. *Z. Anorg. Allg. Chem.* **1957**, *291*, 12.
(7) Juza, R.; Wehle, V. *Naturwissenschaften* **1965**, *52*, 537.
(8) Atoji, M. *J. Chem. Phys.* **1974**, *60*, 3324.
(9) Friedel R. A.; Retcofsky, H. L. *J. Am. Chem. Soc.* **1963**, *85*, 1300.
(10) Traficante, D. D.; Maciel, G. E. *J. Phys. Chem.* **1965**, *69*, 1348.
(11) Zilm, K. W.; Grant, D. M. *J. Am. Chem. Soc.* **1981**, *103*, 2913.
(12) Cross, V. R.; Waugh, J. S. *J. Magn. Reson.* **1977**, *25*, 225.
(13) Beeler, A. J.; Orendt, A. M.; Grant, D. M.; Cutts, P. W.; Michl, J.; Zilm, K. W.; Downing, J. W.; Facelli, J. C.; Schindler, M. S.; Kutzelnigg, W. *J. Am. Chem. Soc.* **1984**, *106*, 7672.
(14) Pines, A.; Gibby, M. G.; Waugh, J. S. *Chem. Phys. Lett.* **1972**, *15*, 373.
(15) Haworth, D. T.; Wilkie, C. A. *J. Inorg. Nucl. Chem.* **1978**, *40*, 1689.
(16) Lewis, W. B.; Rabideau, W.; Krikorian, N. H.; Witteman, W. G. *Phys. Rev.* **1968**, *170*, 455.
(17) (a) Carr, H. Y.; Purcell, E. M. *Phys. Rev.* **1954**, *94*, 630. (b) Becker, E. D.; Ferretti, J. A.; Gupta, R. K.; Weiss, G. H. *J. Magn. Reson.* **1980**, *37*, 381.

Table II. ^{13}C Chemical Shieldings of Inorganic Acetylides and Alkynes

compd	isotropic shift	chem shielding[a] σ_{11}	σ_{22}	σ_{33}	line broadening, kHz fitted[b] a, b	^{13}C–M dipolar coupling[c]	T_1, s
Li_2C_2	195 ± 10	343 ± 15	297 ± 15	−55 ± 25	0.69, 2.71	0.28	360 ± 50
Na_2C_2	170 ± 3	308 ± 5	274 ± 5	−67 ± 5	0.47, 0.52	0.37	30 ± 5
CaC_2	200 ± 5	315 ± 7	315 ± 7	−30 ± 5	1.42, 0.98	0.01	50 ± 10
SrC_2	212 ± 3	318 ± 5	318 ± 5	−1 ± 5	0.47, 0.60	0.05	40 ± 5
BaC_2	229 ± 2	320 ± 3	320 ± 3	50 ± 3	0.21, 0.55	0.13	35 ± 5
C_2H_2[d]	70 ± 3	150 ± 3	150 ± 3	−90 ± 3			
HC≡C—C≡CH[e]	66 ± 1	138 ± 5	138 ± 5	−80 ± 5			
$CH_3C^*{\equiv}CH$[f]	69	140 ± 3	140 ± 3	−74 ± 3			
$CH_3C{\equiv}C^*H$[f]	80	166 ± 3	166 ± 3	−93 ± 3			
$CH_3C{\equiv}CCH_3$	91 ± 8[g]	158 ± 6[g]	158 ± 6[g]	−44 ± 17[g]			
	76 ± 3[f]	152 ± 3[f]	152 ± 3[f]	−75 ± 3[f]			

[a] In ppm, relative to tetramethylsilane (TMS). [b] Coefficients of the inhomogeneous broadening function, $a + b \cos \theta$. [c] Square root of the second moment of the heteronuclear coupling, from the Van Vleck formula (see ref 24). [d] At 20 K, from ref 11. [e] At 163 K, from ref 12. [f] At 20 K, from ref 13. [g] At 87 K, from ref 14.

left (more positive) and the isotropic shift of benzene is at +128.7 ppm.

The metallic nature of some samples (especially Li_2C_2 and SrC_2) caused large changes in the inductance of the NMR sample coil and degraded the matching of the tuned rf circuitry. Consequently, the rf field of the excitation pulses ranged from 110 G for Na_2C_2 to a low of 30 G for Li_2C_2. However, in each case, the pulses were sufficiently intense to probe the frequency range of 1000 to −600 ppm, relative to TMS, with less than 2% intensity loss at the extremes.

Finally, it is noted that certain samples of acetylides are apparently coherers,[18] which complicated the tuning of the resonant circuitry and may have contributed to the causes for the weak NMR signals observed previously.[15] A coherer is typically a metallic particle with an oxidized surface such that a powder of these particles is electrically insulating at low voltages. However, when a sufficiently large voltage is applied across the powder, the particles cohere and the powder becomes electrically conductive. Although the mechanism is unknown, it is proposed that microwelds are formed at contact points. The sample may be restored to the original insulating state by rearranging the particles, such as by shaking or tapping the container. Li_2C_2 and SrC_2 were observed to be extremely sensitive coherers. The electric field induced by a rf pulse of duration 2 μs was sufficient to cohere the particles and detune the probe. The tuning could be restored by lightly tapping the sample, but it was impractical to readjust the sample after each cycle. Instead, it was simpler to prepulse the samples and then retune the NMR probe.

Experimental Results

The ^{13}C NMR spectra of three alkaline-earth-metal acetylides are shown in Figure 2. The principal components of the chemical shielding were obtained from these spectra by least-squares fits to the theoretical expression for the orientational dependence of the chemical shielding.[19] The calculated line shapes, shown by the solid lines in Figure 2, were obtained by convoluting a broadening function into the powder patterns, to be described later. Each spectrum in Figure 2 could be fit with two independent shielding components; the marginally improved fits obtained with three shielding components were statistically insignificant. The degeneracy of two of the shielding components is consistent with the 4-fold rotational symmetry of these acetylides. The shielding parameters and spin–lattice relaxation times are listed in Table II with the convention that $\sigma_{11} \geq \sigma_{22} \geq \sigma_{33}$. These components are related to the isotropic shift ($\langle\sigma\rangle$), the anisotropy ($\Delta\sigma$), and the asymmetry (η) as follows:

$$\langle\sigma\rangle = 1/3(\sigma_{11} + \sigma_{22} + \sigma_{33}) \quad (1)$$

$$\Delta\sigma = 3/2(\langle\sigma\rangle - \sigma_{33}) \quad (2)$$

$$\eta = 3(\sigma_{11} - \sigma_{22})/2\Delta\sigma \quad (3)$$

The ^{13}C NMR spectra of two alkali-metal acetylides are shown in Figure 3. The spectrum of Li_2C_2 is anomalous in two regards: the T_1 is ~10 times longer than the other acetylides and the

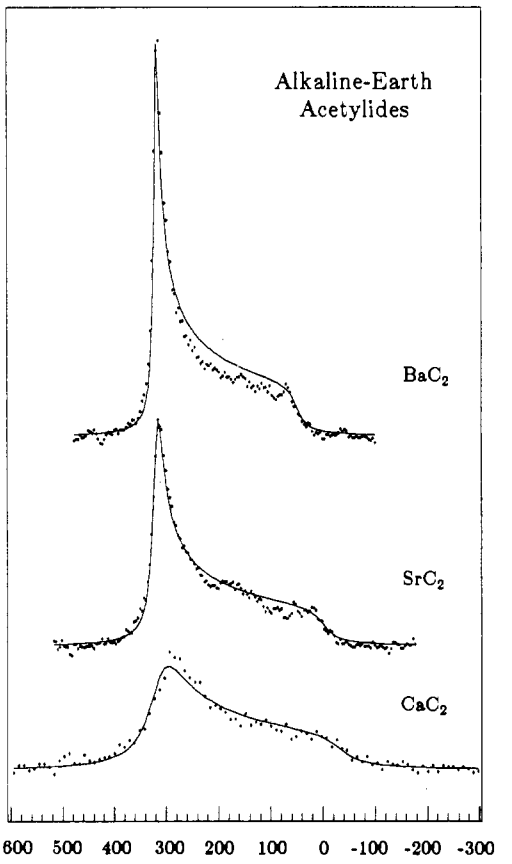

Figure 2. ^{13}C NMR spectra at 20 °C of three alkaline-earth-metal acetylides: CaC_2, SrC_2, and BaC_2. The spectrum of CaC_2 is the accumulation of 126 scans taken at 10.0 min intervals, the spectrum of SrC_2 is the accumulation of 246 scans taken every 3.33 min, and the spectrum of BaC_2 is the accumulation of 280 scans taken every 5.0 min. The chemical shift parameters derived from the fitted lines are summarized in Table II.

spectrum contains an additional feature between the two extreme shieldings. Spectra of similar shape have been reported for other solids and were attributed to orientationally dependent nuclear dipolar couplings[11,20,21] and anisotropic molecular reorientation.[22] Both interpretations are judged to be inappropriate for Li_2C_2 for

(18) Phillips, V. J. *Early Radio Wave Detection*; Peregrinus: New York, 1980.
(19) Haeberlen, U. *High Resolution NMR in Solids: Selective Averaging*; *Advances in Magnetic Resonance, Supp. 1*; Academic: New York, 1976.
(20) VanderHart, D. L.; Gutowsky, H. S.; Farrar, T. C. *J. Chem. Phys.* **1969**, *50*, 1058.
(21) Haubenreisser, U.; Sternberg, U.; Grimmer, A.-R. *Mol. Phys.* **1987**, *60*, 151.
(22) Mehring, M. *Principles of High Resolution NMR in Solids*, 2nd ed.; Springer-Verlag: New York, 1983.

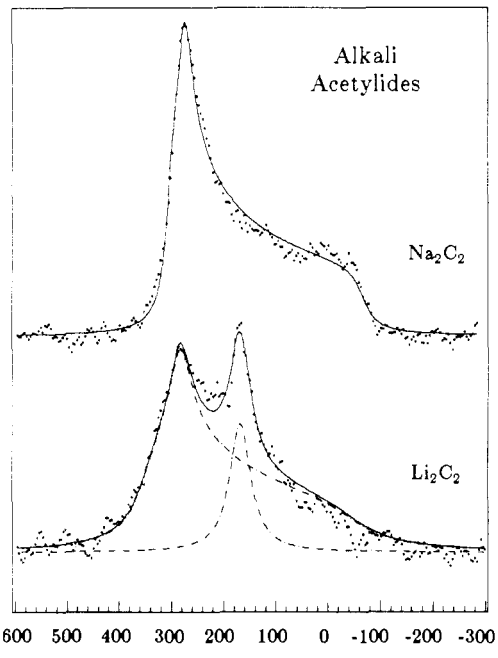

Figure 3. ^{13}C NMR spectra at 20 °C of two alkali-metal acetylides: Li_2C_2 and Na_2C_2. The spectrum of Li_2C_2 is the accumulation of 438 scans taken at 13.3 min intervals and the spectrum of Na_2C_2 is the accumulation of 880 scans taken every 3.33 min. The chemical shift parameters derived from the fitted lines are summarized in Table II.

the following reasons. The effects of orientationally dependent dipolar couplings are observed in the ^{31}P NMR spectrum of $BaPO_3F$,[20,21] which resembles the powder pattern of an axially symmetric shielding with a Lorentzian peak superimposed near the center of mass, similar to the spectrum of Li_2C_2. However, for this effect the dipolar coupling must be comparable to the chemical shift anisotropy and must have a strong orientational dependence. For $BaPO_3F$, the coupling varies from 0 to ~30% of the chemical shift anisotropy.[20,21] For Li_2C_2, the average coupling is only ~3% of the chemical shift anisotropy and varies orientationally by only ~8%. Furthermore, no anomaly is observed in the spectrum of Na_2C_2, which has a structure similar to that of Li_2C_2, and the ^{23}Na–^{13}C coupling is 1.3 times larger than the ^{6}Li,^{7}Li–^{13}C coupling. It is unlikely that the anomaly is caused by librations of the $(C{\equiv}C)^{2-}$ group, because such motion is inconsistent with the long T_1. That is, to cause the observed peak at 170 ppm, the product of the time constant for the molecular reorientation and the chemical shift anisotropy ($\tau_c\Delta\sigma$) would be expected to lie in the range 0.1–1.0. From a general relation for the spin–lattice relaxation owing to chemical shift anisotropy,[23] one predicts a T_1 for Li_2C_2 of 0.3–3.0 s, over 100 times shorter than observed. Of course, this conclusion may be tested by studying the line shape as a function of temperature. (Note that the spectrum in Figure 3 required 4 days of averaging.) The spectrum of Li_2C_2 is assumed to be the sum of two components. The minority species can be fit to a Lorentzian function representing 14% of the integrated area, centered at 169 ppm, of half-width 1.0 kHz (20.5 ppm). The lack of chemical shift anisotropy suggests that this carbon exists in a high-symmetry site. One possibility is a single carbon atom in an acetylide site.

The fits to the spectra of Na_2C_2 and Li_2C_2 showed a statistically significant improvement when the degeneracy of the high-frequency components was lifted. The asymmetry of Na_2C_2 was calculated to be $\eta = 0.14$, and for Li_2C_2, $\eta = 0.18$. This is consistent with the lack of 3-fold (or higher) rotational symmetry in these acetylides. Again, an inhomogeneous broadening function was convoluted into the expression for the chemical shielding.

There are several qualitative trends in the ^{13}C NMR spectra of these acetylides. First, the anisotropies are 15–50% larger than those of organic alkynes. For the five acetylides measured here, $\sigma_\perp$ (or $^1/_2(\sigma_{11} + \sigma_{22})$) is invariant with cation, at ~315 ppm. Conversely, $\sigma_\parallel$ for these compounds spans a range of 115 ppm, generally shifting to lower frequency as the cation size decreases. Two trends are observed in the line broadening: (1) the broadening increases as the cation size decreases and (2) the broadening at $\sigma_\parallel$ is larger than at $\sigma_\perp$, usually by a factor of 2–3. These effects are discussed in the following sections.

It is noted that attempts to obtain ^{13}C NMR spectra of YC_2, LaC_2, and CeC_2 were unsuccessful. No discernible signals were observed for repetition delays up to 15 min with ~100 scans, which produced signals for the five aforementioned acetylides.

Discussion of Results

A. Elements of Chemical Shielding. An external magnetic field perturbs electrons to cause local magnetic fields that shift the resonance frequency of a magnetic nucleus.[24-26] In diamagnetic materials, the dominant effect is a chemical shielding, which Ramsey[27] formulated as a sum of diamagnetic and paramagnetic contributions. For the gauge origin at the observed nucleus, the diamagnetic contribution, σ^d, is caused by magnetic field induced couplings among ground-state electronic wave functions, which causes shifts to lower frequency. The paramagnetic shift, σ^p, results from magnetic field induced couplings to excited states related by angular momentum operators (e.g. $p_x \rightarrow p_y$). Thus, σ^p will dominate in materials with low-lying excited states, relative to kT. Like σ^d, σ^p is proportional to the applied field but conversely causes shifts to higher frequency.

Calculation of the chemical shielding of a nucleus in a solid-state compound is formidable, and one must make approximations to truncate the diverging sum of σ^d and σ^p at large distances. Although the predictions of chemical shielding tensors of small organic molecules has become possible, predictions for bulk solids are less reliable. However, the formalism is useful for the interpretation of relative changes in chemical shieldings. For low-atomic-number nuclei, the contribution from σ^d may exceed that from σ^p, particularly for ionic species and highly polarized molecules.[13] However, chemical shift differences among a series of chemical homologues are usually dominated by changes in σ^p; σ^d is essentially constant.[28,29] This is observed for ^{19}F in CaF_2 as a function of pressure,[30] for ^{13}C in transition-metal carbonyls,[29] and for ^{13}C in linear and pseudolinear molecules.[13] Also, for molecules with C_∞ symmetry, the contribution from σ^p vanishes when the symmetry axis is aligned with the external magnetic field.[31]

B. Analysis of Chemical Shifts in Acetylides. A discussion of the chemical shifts of acetylides is best prefaced by a conclusion of a study of metal carbonyls:[29] "qualitative discussions of ^{13}C shifts are not likely to be successful because of the necessity of taking into account [the average excitation energy, the mean inverse-cubed radius of 2p orbitals, and bond-order terms.] Calculations of the electronic bands and refinement of a method

(23) Wolf, D. *Spin-Temperature and Nuclear-Spin Relaxation in Matter: Basic Principles and Applications*; Clarendon: New York, 1979.
(24) Abragam, A. *The Principles of Nuclear Magnetism*; Oxford Press: London, 1961.
(25) Slichter, D. P. *Principles of Magnetic Resonance*; 2nd ed.; Springer-Verlag: New York, 1978.
(26) Jameson, C. J.; Mason, J. The Chemical Shift. *Multinuclear NMR*; Mason, J., Ed.; Plenum Press: New York, 1987; Chapter 3.
(27) Ramsey, N. F. *Phys. Rev.* **1960**, *78*, 1263.
(28) Pople, J. A. *Mol. Phys.* **1964**, *7*, 301.
(29) Brown, D. A.; Chester, J. P.; Fitzpatrick, N. J.; King, I. J. *Inorg. Chem.* **1977**, *16*, 2497.
(30) Lau, K. F.; Vaughan, R. W. *J. Chem. Phys.* **1976**, *65*, 4825.
(31) Buckingham, A. D.; Malm, S. M. *Mol. Phys.* **1977**, *22*, 1127.
(32) *Handbook of Chemistry and Physics*, 59th ed.; CRC Press: West Palm Beach, FL, 1978.
(33) Kalinowski, H.-O.; Berger, S.; Braun, S. *Carbon-13 NMR Spectroscopy*; Wiley: New York, 1988.
(34) Beagley, B.; Ulbrecht, V.; Katsumata, S.; Lloyd, D. R.; Connor, J. A.; Hudson, G. A. *J. Chem. Soc., Faraday Trans. 2* **1977**, *73*, 1278.
(35) Kalabin, G. A.; Proidakov, A. G.; Radchenko, S. I. *Zh. Org. Khim.* **1980**, *16*, 512.

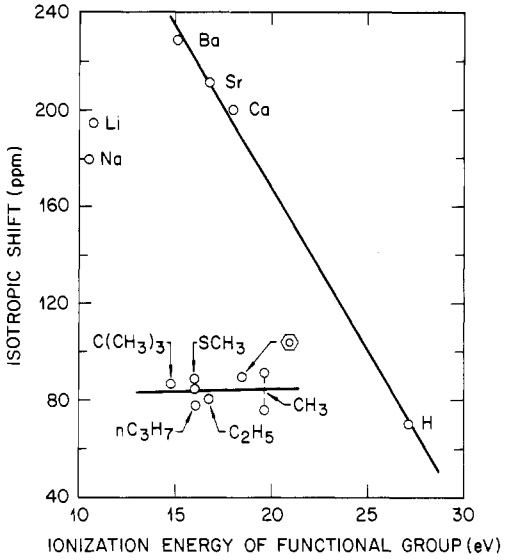

Figure 4. ^{13}C isotropic shifts of acetylenic species as a function of ionization energy of the functional group to which it is bonded. The ionization energies (from ref 32) are twice the first ionization potentials for H, Li, Na, and the alkynes, and they are the sum of the first and second potentials for Ca, Sr, and Ba. The isotropic shifts of the alkynes are from ref 33, and that of bis(methylthio)ethyne is from ref 34 and 35.

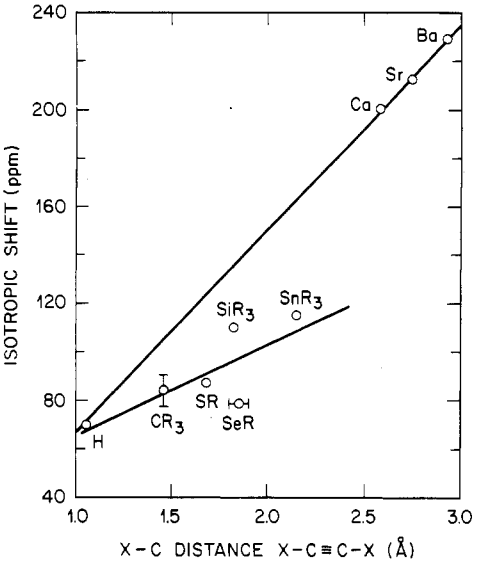

Figure 5. ^{13}C isotropic shifts of acetylenic species as a function of the separation between the carbon atom and the atom along the C≡C axis. The bond lengths are from the following references: H and CR_3, ref 32; SR, ref 34; SeR from $CH_3Se—C{\equiv}N$, ref 41; SiR_3, ref 42; SnR_3, ref 43. The isotropic shifts are from the following references: H, CR_3, SiR_3, and SnR_3, ref 33; SR, ref 34 and 35; SeR, ref 35.

to calculate shifts in solid-state compounds is beyond the intended scope of this paper. This discussion here will entail an examination of relative changes as a function of physical properties. Furthermore, comparisons will be restricted to acetylene compounds with the same functional group attached to each end, to avoid complications caused by polarization of the $(C{\equiv}C)^{2-}$ group.

Figure 4 shows the isotropic shift of acetylene derivatives as a function of ionization energies of the functional group. Clearly, there is no correlation that encompasses all the compounds, although there are trends within subgroups. The isotropic shifts of alkynes are essentially independent of the ionization potential, as shown by a linear regression through this class. The three alkaline-earth-metal acetylides show a linear correlation, which, perhaps fortuitously, extends to C_2H_2, within experimental error. This trend is the same as that observed for the ^{19}F isotropic shift in the series BaF_2, SrF_2, and CaF_2, which was reported as a function of electronegativity.[36] Assuming σ^d is constant, Figure 4 suggests that increased electron donation to the carbon atom, and the attendant changes in crystal structure, increases σ^p for the alkaline-earth-metal compounds; as shown in Figure 1, the alkali-metal acetylides have no on-axis bonding to cations.

The isotropic shift as a function of bond length to the functional group is plotted in Figure 5. The correlation is more monotonic, but again there is no correlation that encompasses all acetylides. The lack of correlation is not surprising considering the diversity of the functional groups. Regression lines are drawn through the two groups of acetylides: those with ionic bonding and those with covalent bonding to the functional group. Again, there is a linear relation between the alkaline-earth-metal acetylides and C_2H_2.

As in the case for Figure 4, the trend for the acetylides shown in Figure 5 is the same as the dependence of ^{19}F chemical shifts on bond lengths reported for alkaline-earth-metal difluorides.[36] However, the trend is the opposite of that reported for chromium carbonyls; decreases in the Cr–C bond length, which was interpreted as causing an increase in metal → carbonyl π back-donation, were accompanied by a shift to higher frequency in the ^{13}C resonance.[37] Although the C≡O unit is isoelectric with $(C{\equiv}C)^{2-}$, a direct comparison may not be appropriate. The trend in carbonyl shifts may be caused by polarization of the carbonyl. For example, trends in ^{13}C shifts in carbonyls are sometimes opposite of trends for ^{17}O.[38]

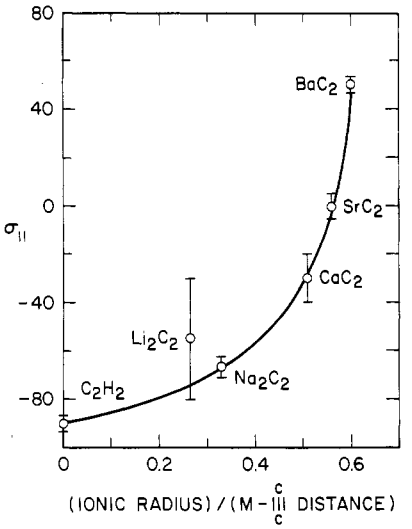

Figure 6. Chemical shielding of acetylides parallel to the applied field, $\sigma_\parallel$, as a function of inverse distance to the nearest neighbor in the plane that bisects the C≡C bond, normalized by the ionic radius of the neighboring atom. The solid line is a spline fit. The distances are calculated from the parameters in Table I, and the ionic radii are from ref 32.

The data in Figures 4 and 5 are plotted against the parameter $\langle\sigma\rangle$, which is more commonly measured and thus allows comparison with a larger number of compounds. However, for the inorganic acetylides, the changes in $\langle\sigma\rangle$ are due to changes in $\sigma_\parallel$; $\sigma_\perp$ is essentially invariant for these compounds.

A previous study showed that $\sigma_\perp$ of linear and pseudolinear molecules is uniformly −90 ppm and off-axis interactions precipitously shift $\sigma_\parallel$ to higher frequency.[13] Figure 6 shows that the same trend is observed for acetylides. For the inorganic acetylides, the amount of off-axis interaction has been expressed as the ratio of the ionic radius of the cation in the plane bisecting the C≡C axis divided by the distance to the C≡C midpoint. This normalized distance should scale with the amount of overlap of the in-plane electronic interactions. Again, there is a correlation that extends to C_2H_2. The correlation suggested in Figure 6 may be useful in analyzing the bonding of acetylides species, for example,

(36) Boden, N.; Kahol, P. K.; Mee, A.; Mortimer, M.; Peterson, G. N. *J. Magn. Reson.* **1983**, *54*, 419.
(37) Bodner, G. M.; Todd, L. J. *Inorg. Chem.* **1974**, *13*, 1335.
(38) Buchner, W.; Schenk, W. A. *J. Magn. Reson.* **1982**, *48*, 148.

adsorbed on surfaces. The orientation of C≡C relative to the surface should strongly influence the position of σ^d.

C. Orientational Dependence of Line Broadening. Derivation of a mathematical expression for the spectral broadening is contingent on identifying its physical origins. Nuclear dipolar coupling is the most common source in spectra of spin-$^1/_2$ nuclei in solids. For acetylides, the ^{13}C dipolar coupling is dominated by heteronuclear interactions; ^{13}C–^{13}C pairs occur for only ~1% of the spins. The ^{13}C–M dipolar couplings are calculated from the Van Vleck formula and are listed in Table II. These are the average broadenings, estimated from the second moment of the heteronuclear couplings. The distribution of cations around the acetylide ion is very symmetric, and consequently the orientational variation of the coupling is less than 10%. Both the magnitude and orientational dependence of the ^{13}C–M nuclear dipolar coupling is insufficient to account for the observed broadening.

Attempts to interpret the orientational dependence in terms of lattice distortions or imperfections were unsuccessful. One might consider a spatial inhomogeneity in the anisotropy caused by impurities or vacancies. This seemingly has potential because $\sigma_\perp$ is insensitive to changes in cation and the orientational factor, $(1 - 3\cos^2\theta)$, is a factor of 2 larger at $\sigma_\parallel$ than $\sigma_\perp$, as observed experimentally. However, this model predicts zero broadening at $\theta = 54.7°$, which causes a node at $\langle\sigma\rangle$ in the simulated spectra. This node is not sufficiently diminished by adding the nuclear dipolar coupling. Since no such feature is observed experimentally, with the possible exception of Li_2C_2, this model is rejected.

In the absence of a physical model, an empirical formula is enlisted. It is found that fits to the spectra are insensitive to how the broadening changes from $\sigma_\perp$ to $\sigma_\parallel$, provided that the change is monotonic. Also, the functional form of the broadening is clearly Lorentzian, as opposed to Gaussian. The broadened spectra shown in Figures 2 and 3 were calculated with

$$I_b(\sigma') = \frac{1}{\pi}\int_{\sigma_\perp}^{\sigma_\parallel} \frac{I(\sigma)\,(\Delta\omega/\omega_0)}{(\Delta\omega/\omega_0)^2 + (\sigma' - \sigma)^2}\,d\sigma \qquad (4)$$

where

$$\frac{\Delta\omega}{\omega_0} = a + \frac{b}{3^{1/2}}\left[1 - \frac{3(\sigma - \langle\sigma\rangle)}{\Delta\sigma}\right]^{1/2} \qquad (5)$$

In eq 4, $I(\sigma)$ is the unbroadened theoretical powder pattern[22] and $I_b(\sigma)$ is the broadened powder pattern. Equation 5 is equivalent to $\Delta\omega/\omega_0 = a + b\cos\theta$, where θ is the angle between the C≡C bond and the applied magnetic field. Fits using eq 5 are slightly better than those obtained using a linearly varying broadening, $\Delta\omega/\omega_0 = a + b(\sigma - \sigma_\perp)/2(\sigma_\parallel - \sigma_\perp)$.

The second trend in the broadening is that the broadening increases as the cation size decreases, as shown in Figures 2 and 3. The amount of braodening is interpreted as the extent of structural inhomogeneity; specifically, as the mean distortion of the C≡C bond from the [001] direction. This interpretation is consistent with the decreasing contribution from σ^p as the cation size decreases, as follows. Burdett and McLarnan studied the progression from CaC_2 to FeS_2 to XeF_2 caused by adding electrons to the anion dimer.[39] Band-structure calculations show that 4 electrons added to a 10-valence-electron unit, a change from $(C{\equiv}C)^{2-}$ to S_2^{2-}, fills π_g^* bands, which stabilizes the deflection of the anion dimer from the [001] direction. Recent calculations of the density of states in acetylides show the dependence on cation in CaC_2 structures.[40] In a comparison of CaC_2 and UC_2, it was shown that increasing the valence-electron count on the C_2 unit from 10 to 12 decreases the gap to the unoccupied states from 2 to 0 eV.[40] By analogy, one would predict a similar, albeit much smaller, trend across the series CaC_2, SrC_2, BaC_2. As the gap decreases, the increased coupling to excited states favors alignment with the [001] direction. Therefore, with this model, it is proposed that from CaC_2 to BaC_2 there is an increased contribution from σ^p and less orientational inhomogeneity.

Summary

Although the $(C{\equiv}C)^{2-}$ ion is relatively invariant between acetylides, having a constant C–C bond length of about 1.19 Å, the ^{13}C NMR spectrum exhibits systematic changes. The linear relations between the isotropic chemical shift and two physical parameters, the cation ionization potential and the cation–acetylide distance, suggest that the $(C{\equiv}C)^{2-}$ unit in inorganic acetylides is similar to that in covalently bonded C_2H_2, but dissimilar from alkynes and acetylene derivatives. The position of the chemical shielding parallel to the C≡C axis is a sensitive indicator of the extent of off-axis bonding and may be useful in the characterization of surface acetylide structures. The spectral broadening is uniformly larger at $\sigma_\parallel$ than at $\sigma_\perp$. This orientational dependence was not interpreted, although it was determined to be not caused by nuclear dipolar couplings. The broadening was also larger for inorganic acetylides with smaller cations, interpreted as larger deviations of the C≡C bond from the [001] axis.

Acknowledgment. Dean Douglass offered insightful comments and suggestions on the origins of the spectral broadening.

(39) Burdett, J. K.; McLarnan, T. J. *Inorg. Chem.* **1982**, *21*, 1119.
(40) Li, J.; Hoffmann, R. *Chem. Mater.* **1989**, *1*, 83.
(41) Marsden, C. J.; Sheldrick, G. M. J. Mol. *Struct.* **1971**, *10*, 413.
(42) Zeil, W.; Harse, J.; Dakkouri, M. *Discuss. Faraday Soc.* **1969**, *47*, 149.
(43) Khaikin, L. S.; Novikov, V. P.; Vilkov, L. V. *J. Mol. Struct.* **1977**, *42*, 129.